Journal of Rehabilitation in Civil Engineering 6-2 (2018) 29-42

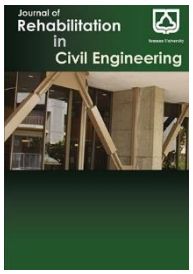

journal homepage: http://civiljournal.semnan.ac.ir/

Ultra-Low Cycle Fatigue Fracture Life of a Type of Buckling Restrained Brace

N. Hoveidae*
*Assistant Professor, Civil Engineering department, Azarbaijan Shahid Madani University, Tabriz, Iran

Corresponding author: *Hoveidaei@azaruniv.ac.ir*

ARTICLE INFO

Article history:
Received: 05 May 2017
Accepted: 05 September 2017

Keywords:
Buckling Restrained Brace,
Ultra-Low Cycle Fatigue,
Cyclic Void Growth Model,
Finite Element Analysis.

ABSTRACT

Buckling restrained braced frames (BRBFs) are considered as popular seismic-resistant structural systems. A BRB sustains large plastic deformations without brace buckling. The core of a buckling restrained brace is prone to fatigue fracture under cyclic loading. The earthquake induced fracture type of the core plate in a buckling restrained brace can be categorized as ultra-low cycle fatigue fracture. This paper investigates the ultra-low cycle fatigue fracture life of a type of composite buckling restrained brace previously tested. The newly developed cyclic void growth model was adopted to theoretically predict the fracture and crack initiation in the core. In addition, the Coffin-Manson fatigue damage model was applied to estimate the fracture life of the brace. A FEM model of the BRB developed in ABAQUS was used to evaluate the fatigue life. The analysis results showed that the cyclic void growth model is capable to nearly predict the fracture life of the core in buckling restrained brace.

1. Introduction

Recently, Buckling Restrained Braced Frames (BRBFs) are considered as popular seismic-resisting structural systems. A BRBF is distinguished from ordinary buckling type brace, where the its buckling is inhibited by a restraining member. There are different details for BRBs including all-steel and composite BRBs. The cyclic response of a BRB is more stable. BRBs are famous for their higher ductility capacity. The ductility in a BRB is produced by plastic deformation of core member without significant local and global buckling of the brace. Many researches have been conducted on seismic response of BRBs which can be found in the works by Black et al. [1], Inou et al. [2], Qiang [3], Watanebe et al. [4], Tremblay et al. [5], Usami et al. [6,7], Hoveidae et al. [8-10], Chou et al. [11], Eryasar et al. [12]. Fig. 1 illustrates the typical BRB detail. The encasing member in a BRB inhibits the brace global buckling and minimizes the core local buckling.

A variety of arrangements have been proposed for BRBs. Hoveidae et al. [10] proposed a novel all-steel BRB in which a shorter core plate was used and then the seismic response of SCBRB was evaluated through nonlinear time history and finite element analyses. Bazzaz et al. [13] proposed a new type of non-buckling steel ring dissipater in off-center and centric bracing systems in order to enhance the ductility of braced system. Moreover, Bazzaz et al. [14] investigated the behavior

DOI: 10.22075/JRCE.2017.11262.1185

of off-center bracing system with ductile element. Andalib et al. [15] analytically and experimentally studied the usage of steel rings made of steel pipes as an energy dissipater at the intersection of braces. These studies showed that the brace with the steel ring exhibits a steady and wide hysteresis curve and a tensile ductility factor of 8.68 was achieved. Furthermore, Bazzaz et al. [16] proposed a new bracing system using circular element (circular dissipater). The analytical results and comparison between plots of these two models showed that the first model has higher performance than the others.

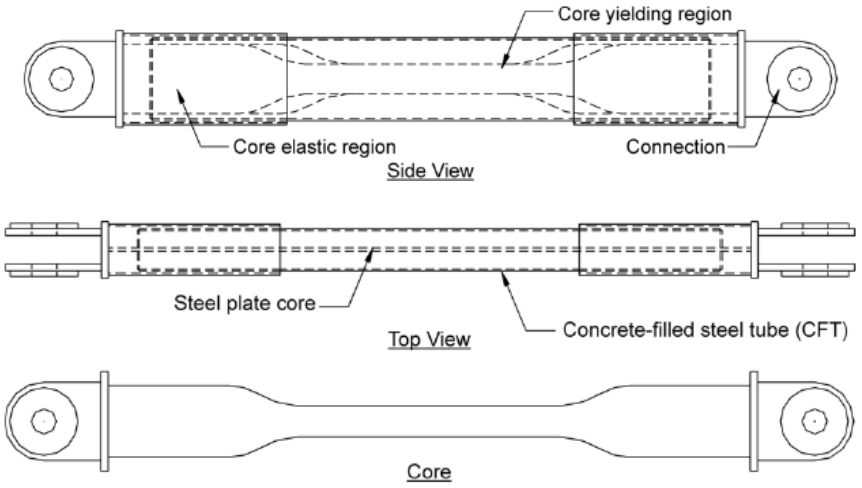

Fig. 1. Typical configuration of a BRB

Ozcelik et al. [17] investigated the response of BRBs with different types of restraining members. It was found that the energy dissipation capacity of BRBs considerably depends on compression strength adjustment factor, β, and strain hardening adjustment factor, ω.

Razavi et al. [18] proposed reduced length buckling restrained brace (RLBRB), in which a shorter core was sandwiched between a restraining member. The test results indicated that the reduction in BRB core length and consequently the increase in strain of core up to amplitudes of 4-5% enhance the risk of low-cycle fatigue failure. The low cycle fatigue response of the core plate was examined by Coffin-Manson fatigue damage criteria as well. Wang et al. [19] surveyed the low cycle fatigue behavior of all-steel buckling restrained braces. Experimental and numerical studies on the effect of stoppers on the low-cycle fatigue performance of buckling-restrained brace to develop the high-performance BRB used in bridge engineering were conducted. According to the mentioned experimental results, the BRBs with stoppers possess a higher low-cycle fatigue performance than those without stoppers.

Yan-Lin et al. [20] proposed core-separated BRBs and theoretically and experimentally investigated the behavior of the brace. It was found that the proposed detail improves flexural rigidity of the restraining system.

Most of research areas in the literature focuses on seismic response of BRBs and the lack of studies on low cycle fatigue response of BRBs is evident.

Typically, a core plate in a BRB is made up of a ductile steel rectangular plate. The core plate is normally designed according to code-based forces. In general, the limit state of a BRB is the core fracture at mid-

length or at the core ends close to transition zones, depending on core details. If a stopper is provided on the core plate to prevent the slippage of restraining member, the core plate tensile fracture is likely to take place at a region near to the stopper [11]. However, in some cases, especially for the BRBs without stopper, the fracture tends to attend the core ends [18]. The fracture of the core plate in a BRB can be classified as a low cycle fatigue or ultra-low cycle fatigue fracture problem, depending on the loading history applied.

Normally, the fracture of steel material under extreme loads occurs at small number of cycles (less than 100 cycles). This fatigue regime is called ultra-low cycle fatigue (ULCF) [21]. The steel damage induced by earthquake can be classified as ultra-low cycle fatigue (Shimada et al. [22], Kuroda [23], Nip et al. [24]), which is categorized by large plastic strains and few cycles to fracture (Zhou et al. [25]). The ULCF fracture is often the governing limit state in steel structures subjected to severe earthquakes. The extremely random loading histories of ULCF associated with very few cycles make them difficult to adapt to techniques developed for high and low cycle fatigue, such as rain-flow cycle counting method (Downing et al. [26]) and strain-life approaches proposed by Manson [27] and Coffin [28].

A number of fatigue damage models, proposed by various authors are available in the literature. ULCF prediction models are usually categorized into two coupled and uncoupled models. An example of coupled plasticity-damage models was proposed by Lemaitre [29]. An exponential ULCF damage rule was proposed by Xue [30] which is more accurate for life prediction in ULCF regime, compared to well-known Coffin−Manson approach (Pereira et al. [21]).

Kanvinde and Deierlein [31] proposed another micro-mechanical based ULCF model based on the cyclic behavior of micro-voids, which enters the stress triaxiality effects into material degradation. The model was called Cyclic Void Growth Model (CVGM). Based on this model, void growth and shrinkage lead to ductile fracture initiation during cyclic loading of the material. This model was verified for several steel types, geometries and loading histories. Despite the low cycle fatigue response of BRBs is investigated in some prior works, which can be found in the literature, the ultra-low cycle fatigue response is not deliberated meticulously. In this paper, the CVGM is applied to a BRB previously tested by Chou et al. [11] in order to predict the ultra-low cycle fatigue life. In addition, the fracture life of the core plate is examined by the well-known Coffin-Manson damage rule and compared with that evaluated by CVGM model.

2. CVGM Formulation

Based on the researches by Kanvinde and Deierlein [31], the two key procedures to capture in ULCF regime are void growth “demand,” including the effects of void growth and shrinkage/collapse, and degraded void growth “capacity,” related to cyclic strain concentrations of the inter void ligament material. The CVGM model proposed by Kanvinde and Deierlein improves the concepts described by Rice and Tracey [32], Hancock and Mackenzie [33] for monotonic loading, and Ristinmaa [34] and Skallerud and Zhang [35] for cyclic loading. The fundamental mechanisms of low cycle fatigue fracture involve cyclic void growth, collapse, and distortion. Fig. 2 represents the ductile fracture mechanism in metals based on

CVGM model. In addition, a fractograph of ULCF is displayed in Fig. 3 [36].

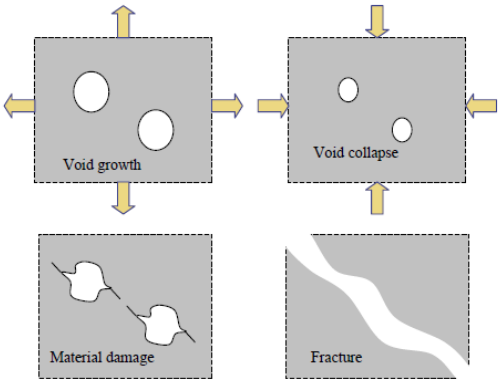

Fig. 2. Micromechanism of ULCF

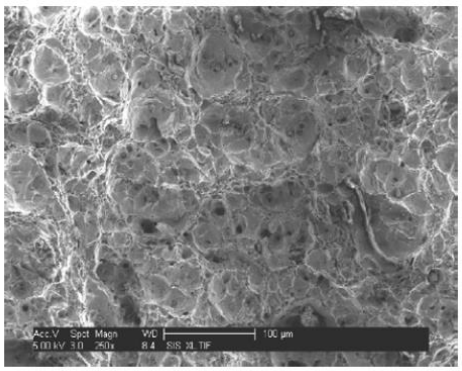

Fig.3. Fractograph of ULCF

First, this paper aims to briefly review the components of CVGM model. The void growth rate can be designated by the next equation for a single spherical void, (Rice and Tracey, [32]):

$$\frac{dR}{R} = C\exp(1.5T)d\varepsilon_p \quad (1)$$

where R is the average void radius; T represents the stress triaxiality which is the ratio of mean stress to effective stress and C is a material parameter. In addition, $d\varepsilon_p$ denotes the incremental equivalent plastic strain as defined in Eq. (2).

$$d\varepsilon_p = \sqrt{\frac{2}{3}d\varepsilon_{ij}^p d\varepsilon_{ij}^p} \quad (2)$$

By integrating Eq. (2), the void radius can be stated as:

$$\ln\frac{R}{R_0} = \int_0^{\varepsilon_p} C\exp(1.5T)d\varepsilon_p \quad (3)$$

where R_0 denotes the initial void size. As the void growth is considered as the controlling parameter of the damage, fracture is triggered when the void ratio reaches a critical value, i.e.:

$$\ln\frac{R^{critical}}{R_{0\ monotonic}} = \int_0^{\varepsilon_p^{critical}} C\exp(1.5T)d\varepsilon_p \quad (4)$$

In order to show the fracture through a void growth index, the calculations above can be simplified.

($VGI_{monotonic}$), which is compared to its critical value, $VGI_{monotonic}^{critical}$ can be defined

$$VGI_{monotonic} = \int_0^{\varepsilon_p} \exp(1.5T)d\varepsilon_p > VGI_{monotonic}^{critical} = \ln(\frac{R}{R_0})_{monotonic}^{critical} / C$$

as below:

(5)

The relations above state the void growth model and can be used for the damage detection under monotonic loadings. However, for cyclic loading, Kanvinde and Deierlein suggested that the fracture initiates when Eq. (6) is satisfied over the characteristic length l^* [37]:

$$VGI_{cyclic} > VGI_{cyclic}^{critical} \quad (6)$$

Where $VGI_{cyclic}^{critical}$ is the critical cyclic void growth index. Considering void shrinkage during compressive (negative) triaxialities, Eq. (5) has been upgraded to the following form:

$$VGI_{cyclic} = \sum_{\text{Tensile cycles}} \int e^{|1.5T|}d\varepsilon_p - \sum_{\text{Compressive cycles}} \int e^{|1.5T|}d\varepsilon_p \quad (7)$$

It is supposed that the critical cyclic void growth damage index can be assessed from its monotonic counterpart as follows:

$$VGI_{cyclic}^{critical} = VGI_{monotonic}^{critical}.\exp(-\lambda\varepsilon_p) \quad (8)$$

The stress and strain histories obtained from finite element analysis can be used to calculate VGI_{cyclic} demand. The parameter λ is a constant which shows the material damageability.

The proper calibration of $VGI_{monotonic}^{critical}$ and λ parameters ascertains the accuracy of CVGM model. Lacking the data for the characteristic length of the ULCF, Kanvinde and Deierlein [31] adopted those of monotonic ductile fracture.

As discussed earlier, based on CVGM model, during ULCF in steel material, damage initiates when Eq. (6) is met over an element with the characteristic length of l^*. Thereafter, when cracking occurs in an element, adjacent elements become more vulnerable to damage initiation and the process of cracking expedites for them as a redistribution in stress and strain happens in the vicinity of cracking zone [38].

3. Coffin-Manson Damage Model

A well-known relation for estimating the low cycle fatigue fracture life of materials proposed by Coffin [30] and Manson [29] can be expressed as follows:

$$\varepsilon_i = \varepsilon_0 {N_f}^m \quad (9)$$

Eq. (9) is represented by a linear relation in a bi-logarithm diagram, where ε_i and N_f are uniaxial plastic strain amplitude and the number of cycles to failure, respectively. ε_0 is the fatigue ductility coefficient and m is the fatigue ductility exponent. Some authors such as Tateishi et al. [39] have shown that the Coffin−Manson relation over-predicts ULCF. However, this issue is going to be examined in this paper by selecting the fracture life predicted by CVGM as a benchmark. A number of equations can be found in the literature which tries to predict the fracture life of BRBs [19]. In this paper the equation proposed by Nakamura et al. [40] as the most conservative equation is selected to estimate the fracture life of the BRB specimen throughout the loading history.

Whenever the damage index (DI) reaches to unity, Low cycle fatigue fracture triggers. Damage in each loading phase is estimated by dividing the number of cycles at that constant amplitude (n_i) by the number of constant amplitude cycles at that amplitude (N_{fi}) necessary to cause fracture. The damage accumulation is based on Miner's rule. The fracture of the component subjected to different levels of strain demand will occur when the index DI reaches to 1 as follows:

$$\sum \frac{n_i}{N_{fi}} = 1 \quad (10)$$

$$DI = \sum_{i=1}^{N} \frac{n_i}{(\frac{\varepsilon_i}{\varepsilon_0})^{\frac{1}{m}}} \quad (11)$$

Based on the equation proposed by Nakamura et al. [45] the parameters m and ε_0 are set to -0.490 and 0.2048, respectively.

4. Assessment of ULCF in BRBs

As mentioned previously, this paper aims to address the ULCF response of buckling restrained braces through the newly developed CVGM model. By knowing the predicted fracture time by CVGM, the damage index estimated by Coffin-Manson rule is also calculated at threshold of fracture and the ability of this method to capture the fracture in ULCF domain is evaluated. For this purpose, a sample composite buckling restrained brace

recently tested by Chou et al. [11] is considered. In order to implement the CVGM method for fracture prediction of the core plate in the BRB specimen, ABAQUS [41] general purpose finite element software is employed. A Fortran UVARM subroutine is developed to calculate the damage indices at each integration point. Fig. 4 represents the characteristics of the BRB specimen tested by Chou et al. [11]. Table 1 summarizes member size of the BRB specimen. Core plate width, b_c , and thickness, t_c , were 150 mm and 22 mm, respectively. ASTM A36 steel with a nominal yield strength of 250 MPa was specified for the channels as restraining members, and ASTM A572 Grade50 steel was specified for the core, side, and face plates. The specified 28-days concrete strength was 35 MPa. Table 2 summarizes the material properties used in specimen 1. The test set-up of the BRB conducted by Chou et al. [11] is indicated in Fig. 5.

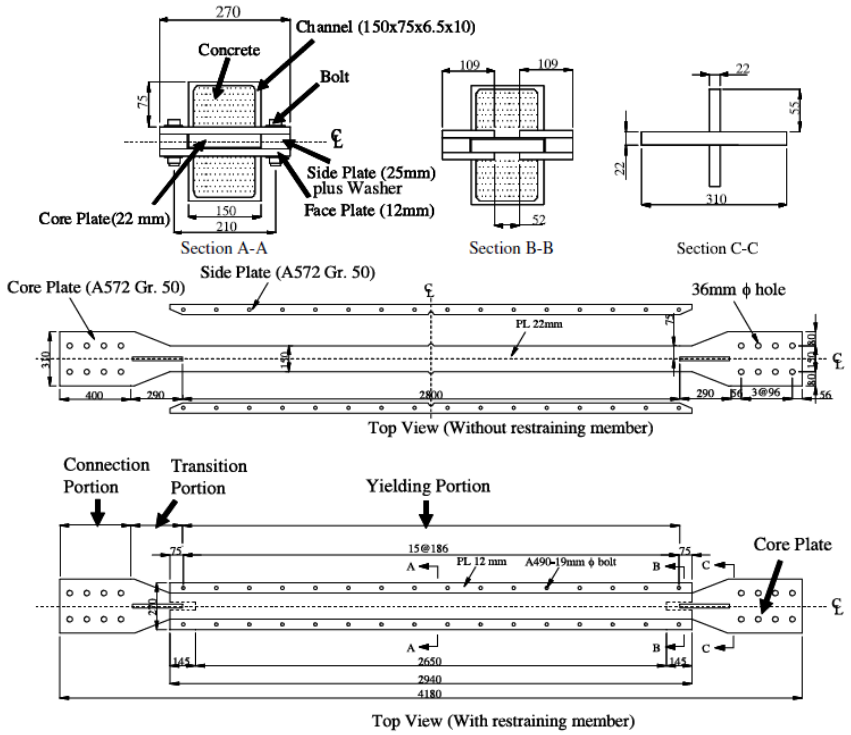

Fig. 4. Details and dimensions of the sample BRB

Table 1. Characteristics of the sample BRB (Specimen-1)

Specimen	Core plate			Channel and face plates(mm)	No. of Bolts	Bolt spacing (mm)
1	b_c(mm)	t_c(mm)	L_y(mm)	150x75x6.5x10	32	186
	150	22	2800	270x12		

Table 2. Material properties of the sample BRB (Specimen-1)

Specimen	Core plate (A572 Gr 50)		Channel		Face plate		Concrete strength (MPa)
1	F_y(MPa)	F_u(MPa)	F_y(MPa)	F_u(MPa)	F_y(MPa)	F_u(MPa)	57
	367	525	274	425	441	565	

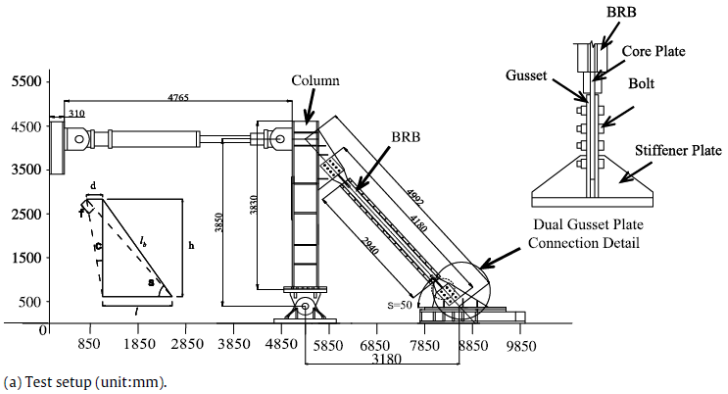

Fig. 5. Test set-up of the sample BRB (Chou et al. 2010)

5. Numerical Modeling of the BRB Specimen

A three dimensional finite element model of the specimen-1 has been considered to assess the applicability of the numerical approach in this paper. The detail and dimensions of BRB model in numerical analysis corresponds to the BRB detail represented in Fig. 4. The connection portion of the braced was eliminated in the FEM model since the brace member was loaded axially. Material nonlinearity with the Von-Mises yielding criterion was considered in the steel core and restraining members. The elastic modulus and the Poisson ratio of steel material were set to 203 GPa and 0.3, respectively. A combined isotropic/Kinematic hardening model represented in Fig. 6a, was used for the steel material in order to accurately capture the cyclic response. The initial kinematic hardening modulus C and the rate factor γ were set to 2 GPa and 12, respectively. The calibration of hardening parameters signified in Fig. 6b, was conducted via comparison between the hysteretic curves obtained from the previous test by Tremblay et al. [5] and the FEM analysis conducted by the author. For isotropic hardening, $Q_{\infty} = 160$ MPa and a rate factor of $b = 5$ were adopted

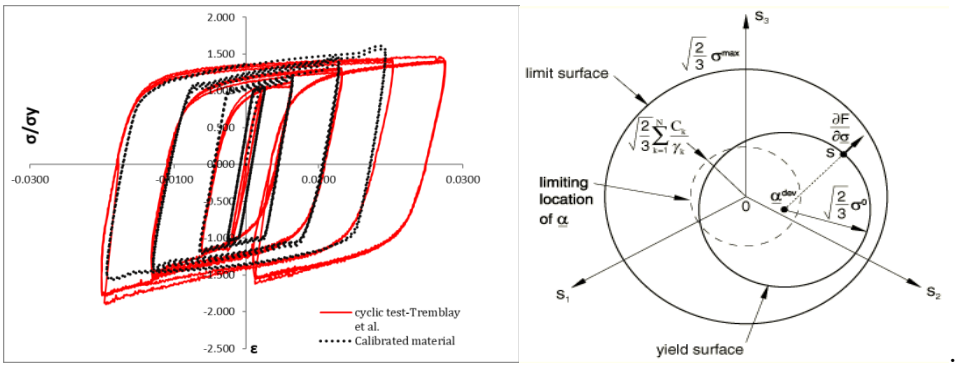

a) b)

Fig. 6. a) 3D representation of the hardening in the nonlinear isotropic/kinematic model; 6b) Material Calibration for A572-Grade50 steel;

Concrete infill as a part of restraining member was modeled with an elastic material with a Young modulus of 25 GPa and a Poisson ratio of 0.2. Other parts of the brace including core plate, restraining channels, and the filler plates were modeled with eight-node solid elements (C3D8R). A fine mesh pattern was introduced in the core plate in order to accurately capture the strain history. However, coarser mesh was assigned to the other parts of the brace because they

were expected to generally remain elastic. A contact interaction was used to capture the interface between the core plate and the restraining member during loading. A friction coefficient of 0.1 was implemented to simulate interface between the core plate and the encasing which is similar to the value adopted in the FEM analysis by Chou et al. [11]. An initial geometric imperfection was introduced in the model based on the data extracted from the first buckling model. The tie interaction was used to model the welding connection of the brace components. The brace was pinned at one core end and the axial displacement history was applied at the other core end. Nonlinear quasi static analysis including both material and geometric nonlinearity and initial and maximum increment size of 0.25 was conducted in ABAQUS 6.13. Full Newton method was assumed as the solution technique.

In this paper, material parameters of CVGM model for the Grade50 steel core including $VGI_{monotonic}^{critical}$ and λ are assumed as 1.13 and 1.18 and the characteristic length l^* was set to 0.18mm, as proposed previously in a paper by Kanvinde and Deierlein [42]. It should be noted that, in the absence of enough laboratory test equipment, it may be possible to use the CVGM parameters based on the values reported in the literature, provided that the specification and mechanical properties of the selected steel material in the analysis and the one formerly calibrated through notched bar tests, closely match together. The ULCF prediction by CVGM model is strongly dependent on key parameters of material specially the $VGI_{monotonic}^{critical}$ amount. Since it is extremely time-consuming to consider the characteristic length l^* for all of the elements in finite element model, only the critical zone in which the fracture is observed in experimental test is modeled with finer mesh. Fig. 7 shows the mesh generation at the critical zone of the core plate. As observed in the test, the core of BRB specimen 1 was fractured at the middle section during the cyclic loading. The BRB specimen in the test was positioned at an inclination of $\theta = 50°$. However, it is modeled horizontally in the finite element program and the corresponding horizontal displacement history is applied at the brace end. The standard and fatigue loading protocols suggested by AISC seismic provisions [43] were applied on BRB model. Standard loading regime was defined at levels corresponding to core strains of 0.33, 0.52, 1.05, 1.58 and 2.1%. After the standard loading, the BRB specimen is subjected to constant-amplitude large deformation demands which is called fatigue test at a core plate strain of 1.6%, up to failure. This type of loading history with large strain amplitudes and limited number of cycles can be classified in ultra-low cycle fatigue domain. Fig. 8 shows the loading protocol applied at the end of BRB model as was used in the test. In addition, Figs. 9a and 9b illustrate the finite element model of the entire BRB and also the restraining member, respectively. Moreover, the finite element model of the core plate and its mesh generation is illustrated in Fig. 10.

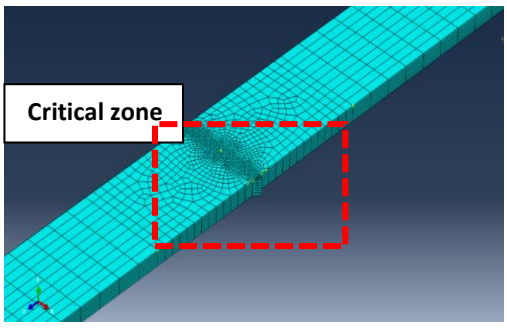

Fig. 7. FE Mesh generation of the BRB core at critical zone

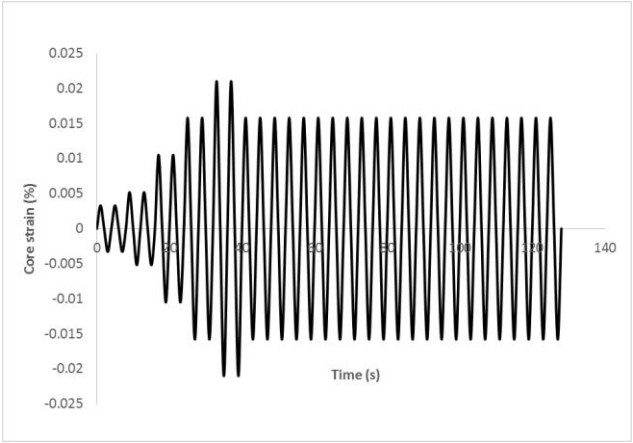

Fig. 8. Applied loading protocol in the BRB test and FEM modeling

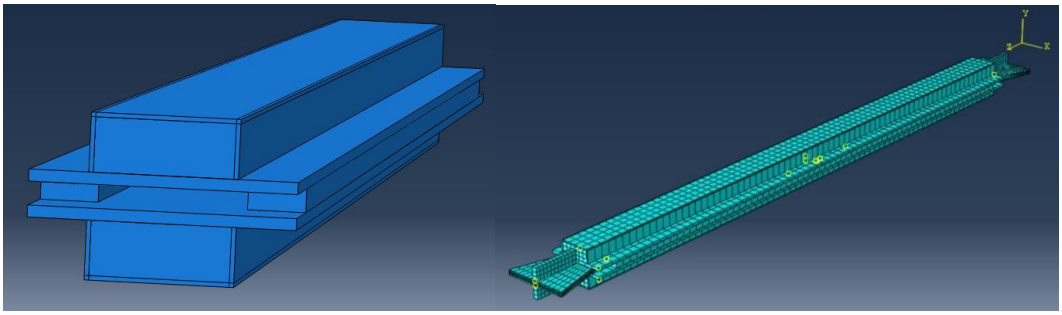

a) b)

Fig. 9. a) FE model of the sample BRB, b) FE model of the restraining parts of BRB core including the channels, filler plates, face plates, and the concrete infill

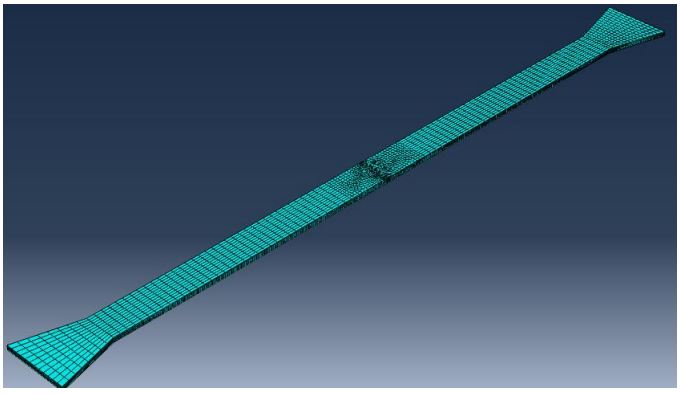

Fig. 10. FE model and mesh generation of the BRB core

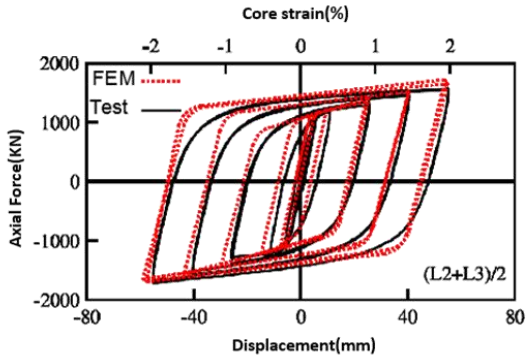

Fig. 11. Comparison of test and FEM hysteretic curves

6. Finite Element Analysis Results

The BRB model was subjected to a cyclic displacement history at the end and the hysteretic response of the brace was captured. Fig. 11 displays the hysteretic response of the BRB model during standard loading protocol and it is compared to the hysteric curve obtained from the test. As shown in Fig. 11, the hysteretic response of the BRB member in the test and the FEM model closely match together and then, the FEM model could properly capture the BRB behavior under prescribed condition and loading history.

As mentioned before, the CVGM is applied to validate the fracture in the BRB specimen. Based on test results, the BRB member tolerated large plastic deformations during standard loading and held a stable hysteretic behavior up to core strain of 2.1%. After the standard loading protocol, the brace was subjected to the fatigue loading sequence with a constant core strain of 1.6% up to failure. The test results showed that the core plate in the BRB specimen was fractured at the mid-section during the low cycle fatigue test and the fracture occurred at the beginning of 22th cycle of low cycle fatigue phase because of the crack initiation and evolution. Remarkably, the CVGM implemented on the FEM model of the BRB specimen is also able to predict the crack initiation and the fracture of the core plate at the same loading sequence and also the same site. The finite element analysis showed that the core fracture starts at the mid-length close to the core stopper. The fracture points in the test and also the FEM model are close together as shown in Figs. 12a and 12b. The contours in Fig. 12b display the UVARM6 field-output which corresponds to the CVGM damage index (i.e. $\frac{VGI_{cyclic}}{VGI_{cylic}^{critical}}$). As shown in Fig. 11b, the damage index evaluated by CVGM at the mid-length of the core and near to the stopper has the maximum value. The fracture is supposed to initiate when the damage index reach to 1. Therefore, the FEM model could properly predict the fracture site. Moreover, the evolution of CVGM demand and capacity over the characteristic length in the core and at the fracture zone is illustrated in Fig. 13. As shown in Fig. 13, the quantity of VGI^{cyclic} capacity decreases based on the accumulation of plastic strain at the beginning of each tensile excursion of loading and the value of $VGI_{cyclic}^{critical}$ increases and decreases based upon the sign of triaxiality. The intersection point of the $VGI_{cyclic}^{critical}$ and VGI_{cyclic} predicts the failure. As revealed in Fig. 13, the intersection point is close to analysis time 125s, which closely coincides with the beginning of the tensile sequence at 22th cycle of the imposed loading history. Therefore, the fracture time closely meet the fracture in the test and the CVGM could properly envisage the failure. Hence, in terms of the fracture site and the time, the FEM model and also CVGM could successfully predict the failure of the BRB in ultra-low cycle fatigue regime. For comparison, the fatigue fracture life of the core plate in the BRB was also estimated by Coffin-Manson relation based on the core strain history during the FEM analysis. The results showed that at the threshold of fracture predicted by CVGM, the Coffin-Manson damage index is just about 0.62 which is remarkably far from 1 (i.e. failure). Therefore, the Coffin-Manson damage criterion seems to overestimate the fracture life of the core plate in the BRB. Such a result can be found in the literature, emphasizing that Coffin-Manson damage

rule can better capture the fracture in low to high cycle damage regimes which should be distinguished from ultra-low cycle fatigue regime.

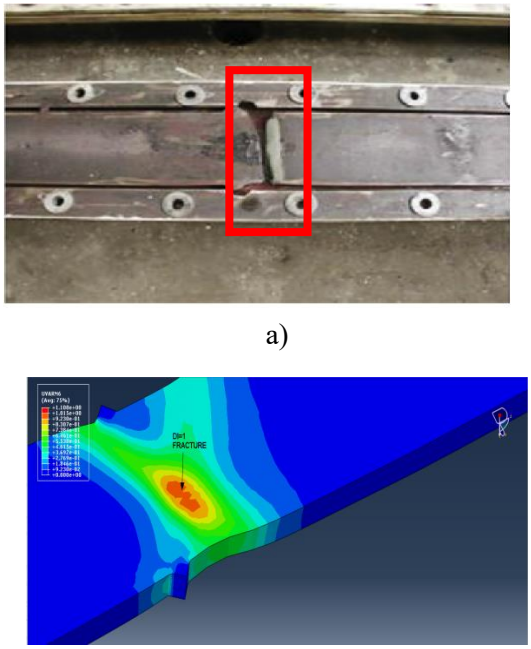

a)

b)

Fig. 12. Critical section of the BRB core in the; a) test; b) FEM model

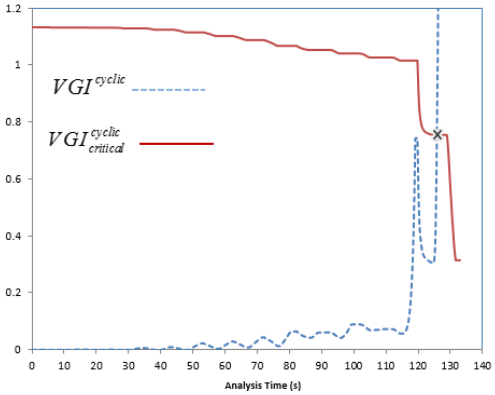

Fig. 13. Comparison of CVGM demand and capacity in FE analysis

7. Conclusions

In this paper, cyclic void growth model (CVGM) as a micromechanical-based fracture model is implemented to validate the ultra-low cycle fatigue fracture life of a buckling restrained brace. The assumed BRB specimen was previously experimentally examined and the fracture was observed after 21 cycles in the low cycle fatigue loading sequence which corresponded to the core strain of 1.6%. In this paper, the Finite element model of the BRB specimen was developed in ABAQUS together with a Fortran subroutine to predict the onset of fatigue fracture in the core. It is observed that the CVGM model is able to successfully predict the fracture initiation in terms of location and time (loading sequence) in the core plate and the results closely meet those observed in the test. As a result, it can be concluded that the cyclic void growth model acts as an acceptable model for predicting crack initiation and the

failure of BRBs (core plate) in ultra-low cycle fatigue regimes. In addition, the results indicated that Coffin-Manson damage rule cannot properly predict the fracture in ultra-low cycle fatigue regime and is likely to overestimate the fracture life. More experimental tests together with FEM analyses are required to validate the CVGM model for ULCF damage prediction of BRBs with different arrangements and details.

REFERENCES

[1] Black, CJ., Makris, N., Aiken, ID. (2002). "Component Testing, stability analysis, and characterization of buckling restrained braced braces". Report No. PEER 2002/08, Univ. of California, Berkeley, CA.

[2] Inoue, K., Sawaizumi, S., Higashibata, Y. (2001). "Stiffening requirements for unbonded braces encased in concrete panels". ASCE Journal of Structural Engineering, Vol.127(6),712-9.

[3] Qiang, X. (2005). "State of the art of buckling-restrained braces in Asia". Journal of Constructional Steel Researches, Vol. 61,727-48.

[4] Watanabe, N., Kat, M., Usami, T., Kasai, A. (2003). "Experimental study on cyclic elasto-plastic behavior of buckling-restraining braces". JSCE Journal of Earthquake Engineering, Vol. 27 [Paper No. 133].

[5] Tremblay, R., Bolduc, P., Neville, R., Devall, R. (2006). "Seismic testing and performance of buckling restrained bracing systems". Canadian Journal of Civil Engineering, Vol. 33(1),183-98.

[6] Usami, T. (2006). "Guidelines for seismic and damage control design of steel bridges". Edited by Japan Society of Steel Construction; Gihodo-Shuppan, Tokyo [in Japanese].

[7] Usami, T., Ge, H., Luo, X. (2009). "Experimental and analytical study on high-performance buckling restrained brace dampers for bridge engineering". Proceeding of 3rd International Conference on Advances in Experimental Structural Engineering, San Francisco.

[8] Hoveidae, N., Rafezy, B. (2012). "Overall buckling behavior of all-steel buckling restrained braces". Journal of constructional steel researches, Vol. (79),151-158.

[9] Hoveidae, N., Rafezy, B. (2015). "Local Buckling Behavior of Core Plate in All-Steel Buckling Restrained Braces". International journal of steel structures, Vol.15(2), 249-260.

[10] Hoveidae, N., Tremblay, R., Rafezy, B., Davaran A. (2015). "Numerical investigation of seismic behavior of short-core all-steel buckling restrained braces". Journal of constructional steel researches, Vol. (114) 89–99.

[11] Chou, C., Chen, S. (2010). "Sub-assemblage tests and finite element analyses of sandwiched buckling-restrained braces". Engineering structures, Vol. 32, Issue 8, Pages 2108–2121.

[12] Eryasar, M., Topkaya, C. (2010). "An experimental study on steel-encased buckling restrained brace hysteretic damper". Journal of Earthquake Engineering Structural Dynamics, Vol. 39, 561-81.

[13] Bazzaz, M., Andalib, Z., Kheyroddin, A. and Kafi, M.A. (2015). "Numerical Comparison of the Seismic Performance of Steel Rings in Off-centre Bracing System and Diagonal Bracing System", Journal of Steel and Composite Structures, Vol. 19, No. 4, 917-937.

[14] Bazzaz, M., Kheyroddin, A., Kafi, M.A., Andalib, Z. and Esmaeili, H. (2014). "Seismic Performance of Off-centre Braced Frame with Circular Element in Optimum Place", International Journal of Steel Structures, Vol. 14, No 2, 293-304.

[15] Andalib, Z., Kafi, M.A., Kheyroddin, A. and Bazzaz, M. (2014). "Experimental Investigation of the Ductility and Performance of Steel Rings Constructed from Plates", Journal of Constructional steel research, Vol. 103, 77-88.

[16] Bazzaz, M., Andalib, Z., Kafi, M.A. and Kheyroddin, A. (2015). "Evaluating the Performance of OBS-C-O in Steel

Frames under Monotonic Load", Journal of Earthquakes and Structures, Vol. 8, No.3, 697-710.

[17] Ozcelik, R., Dikiciasik, Y., Erdil, E. (2017). "The development of the buckling restrained braces with new end restrains". Journal of Constructional Steel Research, Vol. 138, 208-220.

[18] Razavi, A., Mirghaderi, R., Hosseini, A. (2014). "Experimental and numerical developing of reduced length buckling-restrained braces". Engineering Structures, Vol. (77), 143–160.

[19] Wang, C., Usami, T., Funayama, J. (2012). "Improving Low-Cycle Fatigue Performance of High-Performance Buckling-Restrained Braces by Toe-Finished Method". Journal of Earthquake Engineering, Vol. 16,8, 1248-1268.

[20] Yan-Lin, G., Jing, T., Bo-Hao, Z., Bo-Li, Z., Yong-Lin, P. (2017). "Theoretical and experimental investigation of core-separated buckling-restrained braces". Journal of Constructional Steel Research, Vol. 135, 137-149.

[21] Pereira, J., Jesus, A., Xavier, J., Fernandes, A. (2014). "Ultra-low-cycle fatigue behavior of a structural steel". Engineering Structures, Vol. (60), 214–222.

[22] Shimada, K., Komotori, J., Shimizu, M. (1987). "The applicability of the Manson-Coffin law and Miner's law to extremely low cycle fatigue". J Jpn Soc Mech Eng, Vol. 53(491),1178–85.

[23] Kuroda, M. (2002). "Extremely low cycle fatigue life prediction based on a new cumulative fatigue damage model". International Journal of Fatigue, Vol. 24(6), 699–703.

[24] Nip, KH., Gardner, L., Davies, CM. (2010). "Extremely low cycle fatigue tests on structural carbon steel and stainless steel". Journal of Constructional Steel Researches, Vol. 66(1), 96–110.

[25] Zhou, H., Wang, Y., Shi, y., Xiong, J., Yang, L. (2013). "Extremely low cycle fatigue prediction of steel beam-to-column connection by using a micro-mechanics based fracture model". International Journal of Fatigue Vol. 48, 90–100.

[26] Downing, SD., Socie, DF. (1982). "Simple rainflow counting algorithms". International Journal of Fatigue, Vol. 4(1), 31–40.

[27] Manson, SS. (1954). "Behavior of materials under conditions of thermal stress". National Advisory Commission on Aeronautics, Report 1170. Cleveland: Lewis Flight Propulsion Laboratory.

[28] Coffin, Jr. (1954). "A study of the effects of cyclic thermal stresses on a ductile metal". Trans ASME, Vol. 76(6), 931–50.

[29] Lemaitré, J., Chaboche, J-L. (1990). Mechanics of solid materials. Cambridge, UK: Cambridge University Press.

[30] Xue, L. (2007). "A unified expression for low cycle fatigue and extremely low-cycle fatigue and its implication for monotonic loading". International Journal of Fatigue, Vol. 30,1691–8.

[31] Kanvinde, A., Deierlein, G. (2007). "Cyclic void growth model to assess ductile fracture initiation in structural steels due to ultra-low cycle fatigue". Journal of Structural Engineering, Vol. 133(6),701–12.

[32] Rice, J. R., Tracey, D. M. (1969). "On the ductile enlargement of voids in triaxial stress fields". J. Mech. Phys. Solids, Vol. 35, 201–217.

[33] Hancock, J. W., Mackenzie, A. C. (1976). "On the mechanics of ductile failure in high-strength steel subjected to multiaxial stress states". J. Mech. Phys. Solids, Vol. 24,147–169.

[34] Ristinmaa, M. (1997). "Void growth in cyclic loaded porous plastic solid". Mech. Mater., Vol. 26(4), 227–245.

[35] Skallerud, B., and Zhang, Z. L. (2001). "On numerical analysis of damage evolution in cyclic elastic–plastic crack growth problems". Fatigue Fract. Eng. Mater. Struct., Vol. 24(1), 81–86.

[36] Deierlein, G., Kanvinde, A., Myers, A., Fell, B. (2011). "LOCAL CYCLIC VOID GROWTH CRITERIA FOR DUCTILE FRACTURE INITIATION IN STEEL STRUCTURES UNDER LARGE-SCALE PLASTICITY".

Proceeding of EUROSTEEL2011, Budapest, Hungary.

[37] Amiri, H., Aghakoochak, A., Shahbeuk, S., Engelhardt, M. (2013). "Finite element simulation of ultra-low cycle fatigue cracking in steel structures". Journal of Constructional Steel Research, Vol. 89, 175–184.

[38] Afzalan, M., Ghasemieh, M. (2015). "Finite element modeling of failure in steel moment connection subjected to ultra-low cycle fatigue loading". ACEM15, Korea.

[39] Tateishi, K., Hanji, T. (2004). "Low cycle fatigue strength of butt-welded steel joint by means of new testing system with image technique". International Journal of Fatigue, Vol. 26,1349–56.

[40] Nakamura, H., Maeda, Y. & Sasaki, T. (2000). "Fatigue Properties of Practical-Scale Unbonded Braces", Nippon Steel corporations.

[41] ABAQUS (2013). Standard user's manual version 6.13. Providence, RI: Hibbitt, Karlsson & Sorensen Inc.

[42] Kanvinde, A., Deierlein, G. (2006). "The void growth model and the stress modified critical strain model to predict ductile fracture in structural steels". Journal of Structural Engineering, Vol.132(12),1907–18.

[43] AISC (American Institute of Steel Construction), 2010. Seismic provisions for structural steel buildings, Chicago, IL.